Pergamon

*Int. J. Heat Mass Transfer.* Vol. 41, Nos 4–5, pp. 691–697, 1998
© 1997 Elsevier Science Ltd. All rights reserved
Printed in Great Britain
0017–9310/98 $19.00+0.00

PII: S0017–9310(97)00199–3

# Continuous fractional crystallization on a moving cooled belt

P. OSSIPOV

Institute of Mechanical Engineering, Russian Academy of Sciences, Lobachevsky str. 2/31,
P.O. Box 559, 420111 Kazan, Russia

(*Received* 31 *July* 1997)

**Abstract**—Fractional crystallization on cooled surfaces represents a good technique for purifying melts [1–8]. There is a special interest in continuous processes, since they offer several advantages, such as large separation effect, low energy demand, moderate process temperatures and they do not require automation equipment. The understanding of such processes is difficult without a mathematical model which would permit us to evaluate the purity and yield of crystal. There is a good mathematical description of discontinuous fractional crystallization on non-moving cooled walls [9], but this theory is not applicable to continuous processes which employ only moving cooled surfaces (belts). The present article gives a mathematical model for calculating the crystal profile along the belt, crystal purity and its yield. Continuous fractional crystallization on cooled surfaces from a flowing film is a fine technological process, which is much like the crystallization processes used in semiconductor technology. Without understanding the laws which govern the crystal distribution along the belt, one cannot achieve a good yield and purity simultaneously. The suggested model (7)–(11) was successfully tested for dodecanol–decanol mix and for some other substances. This model permits us to investigate the crystal surface stability problem also, which is important at low Reynolds numbers. As a whole, this model gives a powerful tool for optimizating the continuous fractional crystallization process and revealing constructive parameters of the technological equipment. © 1997 Elsevier Science Ltd.

## INTRODUCTION

In recent years fractional crystallization from a flowing film has found extensive use for separation and purification of organic, and inorganic substances in plants worldwide. We will consider only continuous fractional crystallization from a flowing film of liquid. These new processes combine the advantages of crystallization with those of the film-type heat and mass exchange equipment. Typical equipment used in continuous fractional crystallization on cooled surfaces is sketched in Fig. 1.

The melt is fed to the top part of the endless moving belt. The belt slope has the angle $\beta$, therefore, the melt flows down along the belt. The crystal moves with the belt in a countercurrent direction. Crystallization starts with cooling applied to the opposite side of the belt. The process is steady and crystallization occurs continuously. The produced crystal can be essentially more pure than a bulk melt. It is very interesting

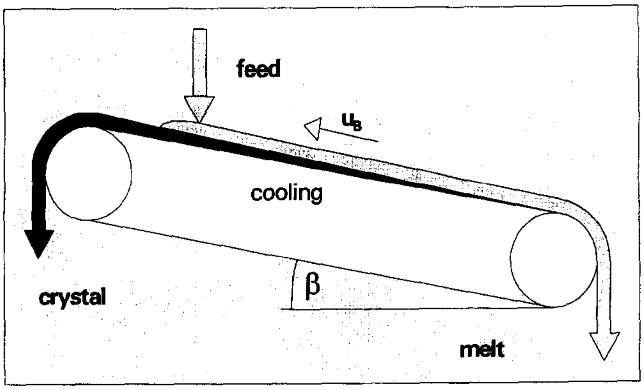

Fig. 1. Scheme of continuous fractional crystallization on the cooled belt.

## NOMENCLATURE

| | |
|---|---|
| $a = \lambda/C/\rho$ | temperature conductivity [$m^2/s$] |
| $b$ | belt width [m] |
| $C$ | melt heat capacity [J/kg/°C] |
| $C_L$ | initial contamination in melt [%] |
| $C_C$ | mean contamination in crystal [%] |
| $D$ | diffusion coefficient [$m^2/s$] |
| $g$ | earth acceleration [$m/s^2$] |
| $H$ | heat of crystallization [J/kg] |
| $K$ | effective distribution coefficient |
| $K_O$ | minimal distribution coefficient |
| $l$ | crystallization length [m] |
| $m$ | mass feed rate [kg/s] |
| $Nu = \alpha \cdot \delta/\lambda$ | Nusselt number |
| $Pr = v \cdot \rho \cdot C/\lambda$ | Prandtl number |
| $Re = V \cdot \delta/v = m/(b \cdot \rho \cdot v)$ | Reynolds number |
| $T_f$ | feed temperature [°C] |
| $T = T(x)$ | mean melt temperature across the film [°C] |
| $T_M$ | melting temperature [°C] |
| $T_O(x)$ | temperature under the belt [°C] |
| $u_B$ | belt speed [m/s] |
| $V$ | mean film speed [m/s] |
| $V_C(x)$ | crystal growth rate [m/s] |
| $x$ | coordinate along the belt [m] |
| $y$ | coordinate across the belt [m]. |

*Greek symbols*

| | |
|---|---|
| $\alpha$ | heat transfer coefficient [$W/m^2/°C$] |
| $\beta$ | belt angle [rad] |
| $\delta$, $\delta_C(x)$, $\delta_B(x)$ | film, crystal and belt thicknesses [m] |
| $\delta_D = \delta_q \cdot (D/a)^{0.344}$ | diffusion layer thickness [m] |
| $\delta_q = \delta/Nu$ | heat layer thickness [m] |
| $\lambda$, $\lambda_C$, $\lambda_B$ | heat conductivities of melt, crystal, belt [W/m/°C] |
| $v$ | kinematic viscosity [$m^2/s$] |
| $\rho$ | melt density [$kg/m^3$]. |

to know the conditions which determine the crystal purity. As a measure of the purity we usually consider the effective distribution coefficient which is equal to the ratio of the impurity concentrations, respectively, in the crystal and in the bulk melt.

## CRYSTAL PURITY AS A FUNCTION OF ITS PROFILE

It is well known that the crystal purity depends considerably on its growth rate [2]. We can write the dependence [10]

$$k = \frac{k_O}{k_O + (1 - k_O) \cdot \exp^{-\delta_D \cdot V_C/D}} \qquad (1)$$

of the effective distribution coefficient $k$ versus crystal growth rate, $V_C$. This dependence shows that the crystal growth rate has a great influence on its purity (Fig. 2). Moreover, it imposes heavy restrictions on the magnitude of the growth rate. So, for most organic and inorganic substances we can attain good purification with growth rate under 1 cm/h [9]. To clarify the importance of the crystal profile we will consider

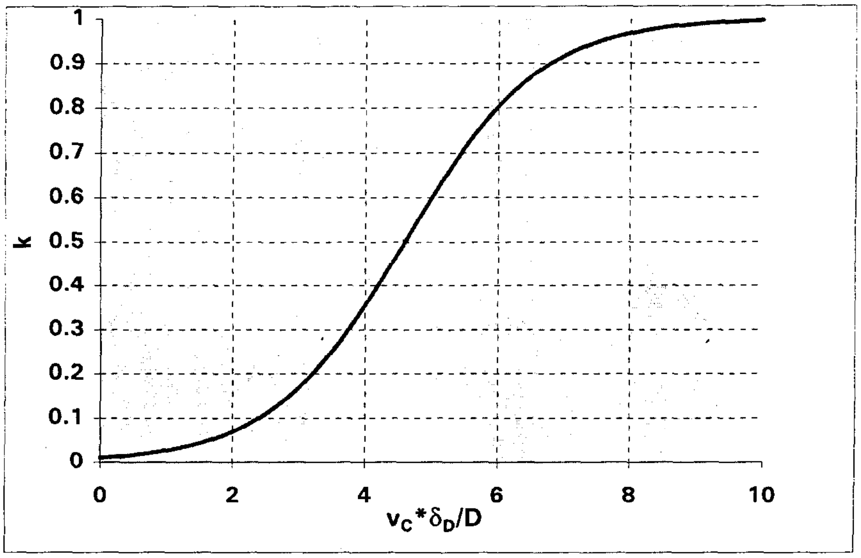

Fig. 2. Distribution coefficient vs crystal growth rate.

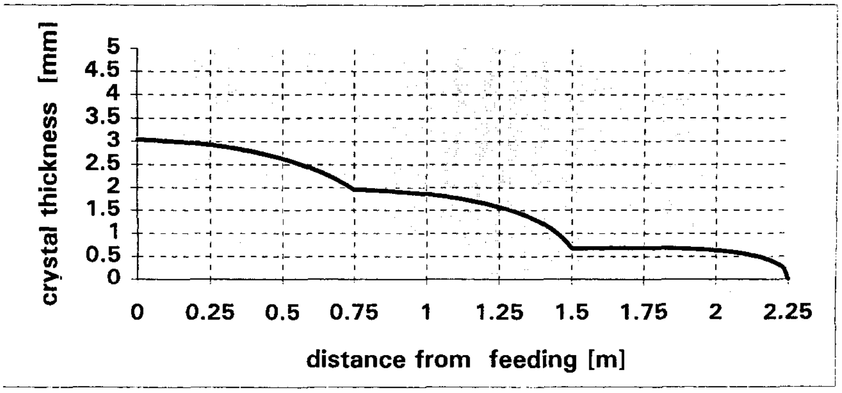

Fig. 3. Crystal profile for different cooling under three zones.

Table 1.

| N zone | Crystal growth rate (cm/h) | Crystal impurity (%) |
|---|---|---|
| 1 | 0.5 | 0.14 |
| 2 | 0.7 | 0.21 |
| 3 | 4.5 | 1.01 |
| Total | 1.7 | 0.52 |

a crystal which is produced in three zones with different cooling temperatures (Fig. 3).

The mean crystal growth rates over each zone are listed in Table 1. We can see that the growth rate differs markedly depending on the zone. As a consequence, the mean surface crystal impurities are also different corresponding to equation (1). Column 2 demonstrates these impurities over all three zones. Thus, for predicting the crystal purity it is very important to know its profile.

## EQUATION FOR CRYSTAL PROFILE

Consider now the stable crystal profile. It is characterised by the distribution of the crystal thickness along the belt $\delta_C(x)$ (Fig. 4). Because of the low speed of the belt, we can make the following assumptions: temperature distributions through the belt and crystal are linear; heat capacities of the belt and crystal are negligible. The other natural assumption [9] is that the temperature at the crystal surface is equal to the equilibrium melting temperature $T_M$. The heat flux from the hot melt to the crystal surface can be written as

$$Q_{M-C} = \alpha \cdot \{T(x) - T_M\}. \qquad (2)$$

The heat flux from the crystal surface toward the belt is equal to

$$Q_{C-O} = \frac{T_M - T_O(x)}{\dfrac{\delta_C(x)}{\lambda_C} + \dfrac{\delta_B}{\lambda_B}} \qquad (3)$$

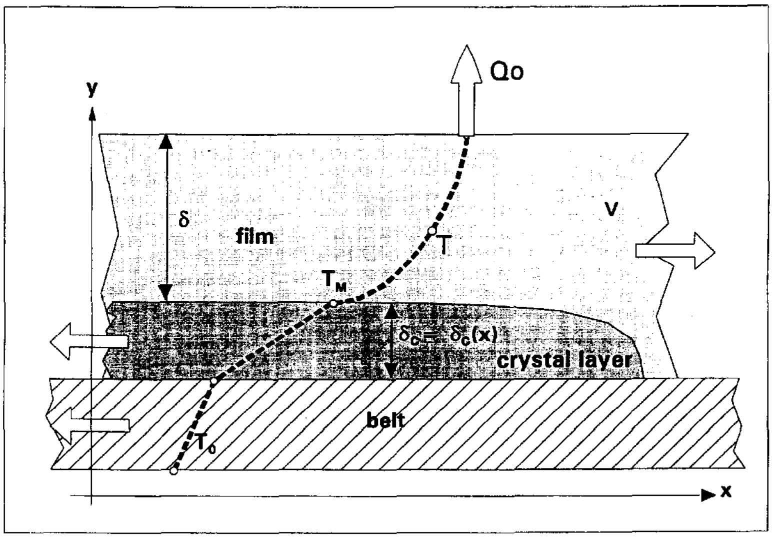

Fig. 4. Heat transfer and temperature distribution across layer.

Because crystallization occurs on the crystal surface, the crystallization heat

$$Q_C = \rho\cdot V_C(x)\cdot H \tag{4}$$

must be taken into account. The difference between the heat fluxes towards the belt and from the melt must be equal to the crystallization heat: thus the heat balance on the crystal–melt interface can be written:

$$Q_{C-O} = Q_C + Q_{M-C}. \tag{5}$$

Since the crystal is usually thin, the growth rate, $V_C(x)$ can be expressed as follows:

$$V_C(x) = -u_B\cdot\frac{d\delta_C(x)}{dx}. \tag{6}$$

Summarizing equations (2)–(6) we obtain the equation:

$$\rho\cdot H\cdot u_B\cdot\frac{d\delta_C(x)}{dx} = \alpha\cdot\{T(x)-T_M\} - \frac{T_M - T_O(x)}{\frac{\delta_C(x)}{\lambda_C}+\frac{\delta_B}{\lambda_B}}$$

or in dimensionless form

$$\frac{\rho\cdot H\cdot u_B\cdot\delta^2}{T_M\cdot l\cdot\lambda}\cdot\frac{d\delta_C^*(x^*)}{dx^*} = Nu\cdot\{T^*(x^*)-1\} - \frac{1-T_O^*(x^*)}{\frac{\delta_C^*(x^*)}{\lambda_C^*}+\frac{\delta_B^*}{\lambda_B^*}} \tag{7}$$

where

$$x^* = \frac{x}{l}$$

$$\delta_C^* = \frac{\delta_C}{\delta} \quad \delta_B^* = \frac{\delta_B}{\delta}$$

$$\lambda_C^* = \frac{\lambda_C}{\lambda} \quad \lambda_B^* = \frac{\lambda_B}{\lambda}$$

$$T^* = \frac{T}{T_M} \quad T_O^* = \frac{T_O}{T_M}.$$

The ordinary differential equation (7) permits us to calculate the crystal thickness $\delta_C^*(x^*)$. The following boundary condition must be taken $\delta_C^*(1) = 0$, in order to ensure the absence of uncontrolled crystal flow at the beginning of the crystallization zone. The three parameters in equation (7) are yet unknown: mean (across film) temperature of the flowing melt film, the film thickness and the Nusselt number.

## FILM TEMPERATURE ALONG THE BELT

The heat balance for the flowing film is

$$\delta\cdot C\cdot\rho\cdot V\cdot\frac{dT}{dx} = -\alpha\cdot\{T(x)-T_M\} - Q_O$$

$Q_O$ is the heat loss with evaporation and convection. Finally, we can write this equation in dimensionless form

$$\frac{dT^*}{dx^*} = -\frac{\{T^*(x^*)-1+T_M^*\}}{L^*} \tag{8}$$

with the characteristic length

$$L^* = \frac{\delta}{l}\cdot Pr\cdot\frac{Re}{Nu}$$

and temperature correction

$$T_M^* = \frac{Q_O\cdot\delta}{Nu\cdot\lambda\cdot T_M}.$$

The value $T_M^*$ does not usually vary significantly, so the solution of (8) can be written:

$$T^* - 1 + T_M^* = \{T_f^* - 1 + T_M^*\}\cdot\exp\left\{-\frac{x^*}{L^*}\right\}$$

where

$$T_f^* = \frac{T_f}{T_M}.$$

In Fig. 5 the film temperature along the belt for dodecanol–decanol mix is depicted.

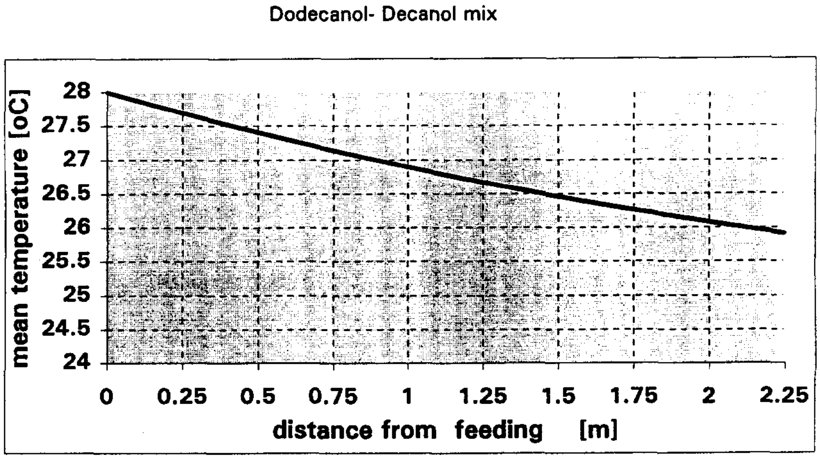

Fig. 5. Mean (across melt) melt temperature along the belt.

## FILM THICKNESS

An exhaustive study of this problem was carried out by Brauer [11]. He showed that the regime of film flow is laminar is $Re < 400$, and turbulent if $Re > = 400$. He suggested the following relation for film thickness in the turbulent mode

$$\delta = 0.302 \cdot \left(\frac{3 \cdot \nu^2}{g \cdot \sin\beta}\right)^{1/3} \cdot Re^{8/15}.$$

An analogous relation for the laminar mode can be obtained from the Navier–Stokes equation

$$\delta = \left(\frac{3 \cdot \nu^2}{g \cdot \sin\beta}\right)^{1/3} \cdot Re^{1/3}.$$

## NUSSELT NUMBER

Both equations (7) and (8) contain the Nusselt number. Wilke [12] made a comprehensive study of heat transfer from a falling liquid film to the surface. He suggested that the local heat-transfer coefficients might be calculated by the following equations for steady flow:

$$Nu = 1.88 \qquad Re < Re^* = 615 \cdot Pr^{-0.646}$$

$$Nu = 0.0614 \cdot Re^{8/15} \cdot Pr^{0.344} Re^* < Re < 400$$

$$Nu = 0.00112 \cdot Re^{6/5} \cdot Pr^{0.344} \quad 400 < Re < 800$$

$$Nu = 0.0066 \cdot Re^{14/15} \cdot Pr^{0.344} \quad 800 < Re.$$

These equations are valid for a smooth surface. In [2, 9] the crystalline layer was shown to display such a surface until dendritic crystal growth began.

## CRYSTAL YIELD AND PURITY

Using equation (7) the value $\delta_C(0)$ and the crystal yield

$$P = \rho \cdot b \cdot u_B \delta_C(0) \tag{9}$$

can be calculated. The knowledge of the crystal profile permits us also to evaluate the mean (across crystal layer) crystal impurity. We will employ the results of earlier investigations [9, 13–16]. According to these results we can use the relations (1) and (6) and write a one-dimensional approximation:

$$C_C = \frac{C_L}{\delta_C(0)} \cdot \int_0^l \frac{k_O}{k_O + (1 - k_O) \cdot \exp^{-(\delta_D \cdot u_B \cdot |d\delta_C(x)/dx|)/D}} \cdot \frac{d\delta_C(x)}{dx} \cdot dx. \tag{10}$$

In our work (in press) it has been shown that the one-dimensional approximation is sufficiently exact in typical cases when the belt length is much more than 0.3 m and the crystal growth rate is changing along the belt by no more than a factor of 2–3. The two-dimensional approach has been suggested, but it is out of the scope of this article. The surface impurity distribution $C_d(x)$ for the crystal profile shown in Fig. 3 is presented in Fig. 6.

We can see the great nonuniformity of impurity along the crystal surface. Eliminating $x$ from the dependencies $\delta_C(x)$ and $C_d(x)$ gives the concentration distribution across the crystal $C_d(\delta_C)$. This distribution shows the great nonuniformity of purity across the crystal (Fig. 7).

## CONSTITUTIONAL SUPERCOOLING

For good purification the crystal surface must be morphologically stable to avoid a great amount of entrainment. The careful study of entrainment influence on the crystal purity is given in articles [4, 5, 9]. We will only note that the crystallization front does not have a cellular or dendritic structure (hence, is morphologically stable) at any point $x$ of crystal surface until the actual temperature gradient in the liquid film at the interface is greater or equal to the equi-

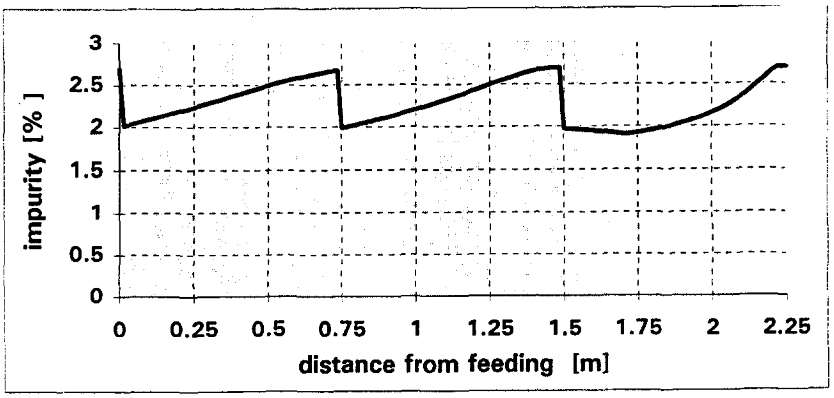

Fig. 6. Surface impurity distribution along the crystal.

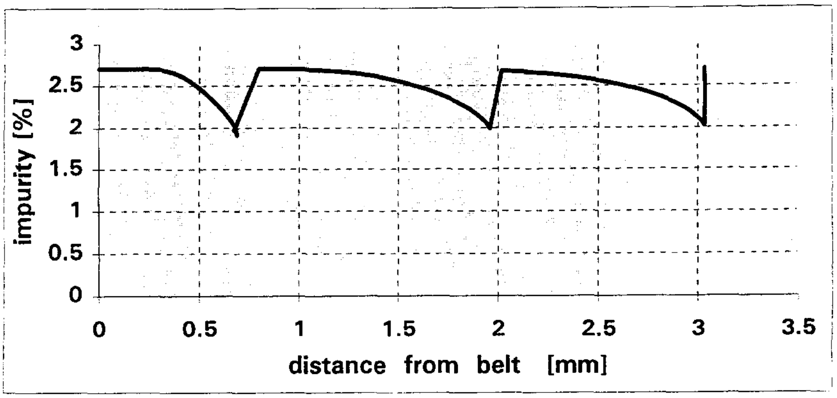

Fig. 7. Impurity distribution across the crystal.

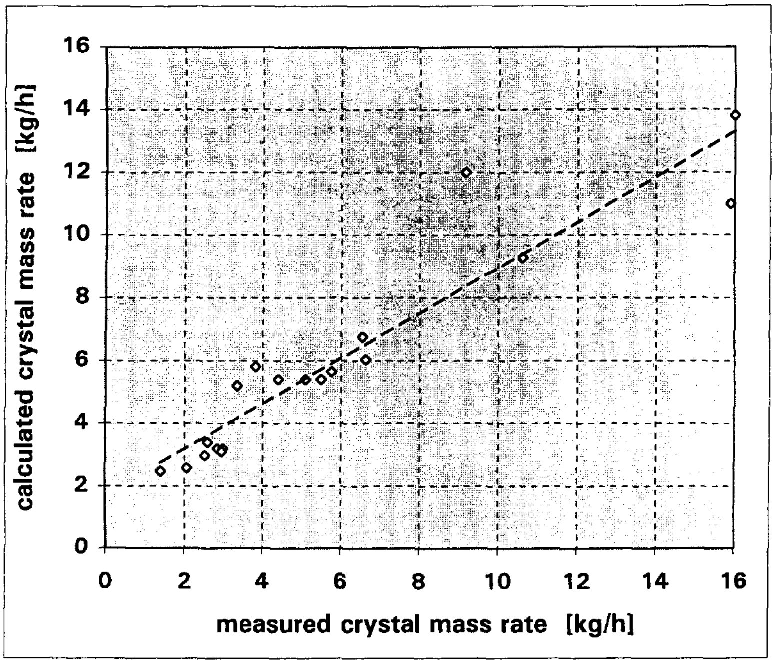

Fig. 8. Comparison between experiment and theory (crystal mass rate).

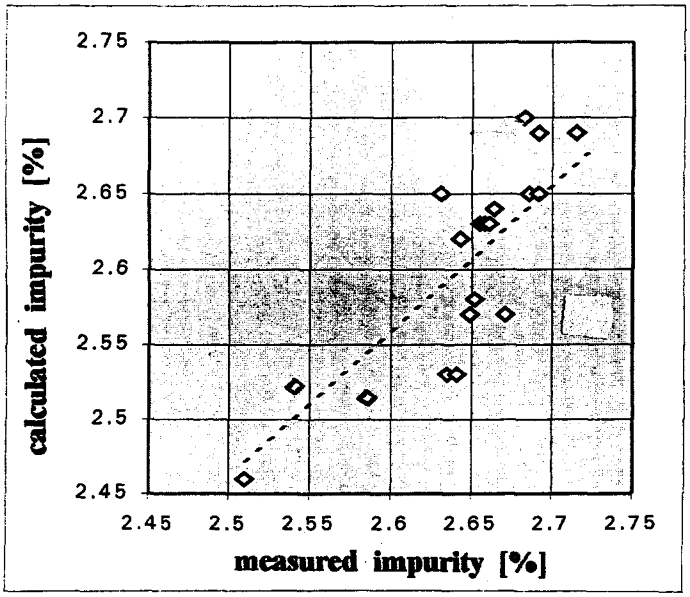

Fig. 9. Comparison between experiment and theory (crystal purity).

librium temperature gradient [9, 16]. Knowledge of the crystal thickness permits us to obtain the criteria for morphological stability of the crystal surface:

$$\frac{T(x)-T_{\mathrm{M}}}{\delta_{\mathrm{q}}} \geqslant \frac{n\cdot u_{\mathrm{B}}\cdot\left|\frac{\mathrm{d}\delta_{\mathrm{C}}(x)}{\mathrm{d}x}\right|\cdot C_{\mathrm{L}}}{D\cdot\left\{k_0/(1-k_0)+\exp\left(-\delta_{\mathrm{D}}\cdot u_{\mathrm{B}}\cdot\left|\frac{\mathrm{d}\delta_{\mathrm{C}}(x)}{\mathrm{d}x}\right|/D\right)\right\}} \tag{11}$$

with $n$ being the slope module of the liquidus curve at bulk contamination $C_{\mathrm{L}}$. Investigations of Hurle in semiconductor technology [16] showed that the crystal surface for sufficient pure melt can be also morphologically stable (without dendrites) in cases when this condition is invalid.

## COMPARISON WITH EXPERIMENT

Numerous experiments were carried out to verify the suggested model. In Figs. 8 and 9 the relations between the measured and calculated crystal yield and purity for dodecanol–decanol mix are depicted. The good agreement proves the validity of the suggested model.

## REFERENCES

1. Wintermantel, K. and Kast, W., Wärme und Stoffaustausch bei der Kristallisation an gekühlten Flächen. *Chemie-Ingenieur-Technik*, 1973, **45**(10), S.284, S.728–731.
2. Wintermantel, K., Die effektive Trennwirkung beim Ausfrieren von Kristallschichten aus Schmelzen und Lösungen—eine einheitliche Darstellung. *Chemie-Ingenieur-Technik*, 1986, **58**(6), S.498–499.
3. Mayer, M., Gerichtete fraktionierte Kristallisation aus dem Rieselfilm. *Verfahrenstechnik*, 1974, **8**(8), S.221–223.
4. Lapin, N., Nikolaev, D., Malyusov, V. and Zhavoronkov, N., Entrainment of the melt in the crystallization of organic systems that form eutectics. *Teoreticheskie Osnovy Khimicheskoi Tekhnologii*, 1976, **10**(1), 31.
5. Lapin, N., Nikolaev, D., Malyusov, V. and Zhavoronkov, N., Entrainment of the melt in the crystallization of organic systems that form solid solution. *Teoreticheskie Osnovy Khimicheskoi Tekhnologii*, 1976, **10**(4), 508.
6. Hünken, I., Ulrich, J., Fischer, O. and König, A., Continuous and countercurrent layer crystallization. *Proceedings of the 12th Symposium on Industrial Crystallization*, Warzaw/Poland, Z.H. Rojkowski (ed.), Vol. 1, 1993, pp. 1.005–1.060.
7. Ulrich, J., Hünken, I., Fischer, O. and König, A., Eine Apparatur zur kontinuerlichen Stofftrennung mittels gerichteter Kristallisation. *GVC-Jahrestreffen der Verfahrensingenieure*, Wien/Austria, 1992, **64**(9), 842–844.
8. Hünken, I., Oezoguz, and Ulrich, J., A new apparatus for a continuous directed crystallization process. *Proceedings BIWIC* 1991 (*Bremer International Workshop for Industrial Crystallization*), Bremen, Germany, J. Ulrich (ed.). Verlag Mainz GmbH, Aachen (ISBN 3-925714-44-8), 1991, pp. 42–49.
9. Myasnikov, S., Kasymbekov, B., Malyusov, V. and Zhavoronkov, N., Theoretical fundamentals of fractional crystallization. *Teoreticheskie Osnovy Khimicheskoi Tekhnologii*, 1984, **18**(6), 749–760.
10. Matz Günther, *Kristallisation*. Springer, Berlin, 1969, 418.
11. Brauer, H., Strömung und Wärmeübergang bei Rieselfilmen. *VDI Forschungsheft*, no. 457, 1956, p. 22.
12. Wilke, W., Wärmeübergang an Rieselfilme. *VDI Forschungsheft*, no. 490, 1962, p. 28.
13. Burton, J., Prim, R. and Slichter, W., The distribution of solute in crystals grown from the melt. *Journal of Chemistry and Physics*, 1953, **21**, 1987.
14. Kulov, N., Murav'ev, M., Malyusov, V. and Zhavoronkov, N., Rate profiles in falling liquid films. *Teoreticheskie Osnovy Khimicheskoi Tekhnologii*, 1982, **16**(4), 499.
15. Lapin, N., Malyusov, V. and Zhavoronkov, N., Calculating the distribution of an impurity in the crystallisation of stirred melts with a cellular crystallization front. *Doklady Akademii Nauk SSSR*, 1981, **256**(3), 650.
16. Hurle, D., Constitutional supercooling during crystal growth from stirred melts. *Solid-State Electronics, Part* 1, 1961, **3**, 37–41.